ELSEVIER

Organic Electronics 3 (2002) 53–63

Organic Electronics

www.elsevier.com/locate/orgel

Electronic structure and current injection in zinc phthalocyanine doped with tetrafluorotetracyanoquinodimethane: Interface versus bulk effects

Weiying Gao, Antoine Kahn *

Department of Electrical Engineering, Princeton Materials Institute, Princeton University, Engineering Quadrangle, 08544-5263 Princeton, NJ, USA

Received 19 November 2001; accepted 4 February 2002

Abstract

The p-type doping of zinc phthalocyanine (ZnPc) with the highly electronegative tetrafluorotetracyanoquinodimethane (F_4-TCNQ) is investigated via direct and inverse photoemission spectroscopy and in situ current–voltage (I–V) measurement. The electron affinity of F_4-TCNQ and the ionization energy of ZnPc are found to be energetically compatible with an electron transfer between the highest occupied molecular orbital (HOMO) of the host and the lowest unoccupied molecular orbital of the dopant. The Fermi level is near mid-gap in undoped ZnPc, and drops to 0.42 and 0.18 eV above the HOMO in the 0.3% and 3% doped films, respectively, consistent with efficient p-doping. The dependence of the Au/ZnPc:0.3%F_4-TCNQ/Au I–V characteristics on the thickness of the organic film is analyzed in terms of injection-limited versus space-charge-limited current. The analysis demonstrates that the large doping-induced increase in hole current is primarily due to improved carrier injection via tunneling through the narrow interface space charge layer.

1. Introduction

Electrical doping of organic molecular films has been investigated relatively little as compared to doping of inorganic semiconductors. The main reason is that, unlike in inorganic semiconductors, traditional n- and p-doping has not been a requirement for achieving bipolar transport in the most common molecular device, i.e. the organic light emitting diode (OLED). The ability to stack *electron transport* and *hole transport* organic layers alleviates the need to "dope" the materials to inject electrons and holes into the active layer(s). However, the performance of organic devices is now reaching levels at which electrical doping looks attractive as a means to further improve efficiency, in particular by enhancing carrier injection and lowering drive voltages. This can be achieved for example by heavy doping of an organic interface to create a narrow depletion region (the depletion region appears as a result of the difference between the interface Fermi level position, which is fixed by

* Corresponding author. Tel.: +1-609-258-4642; fax: +1-609-258-6279.

E-mail address: kahn@ee.princeton.edu (A. Kahn).

1566-1199/02/$ - see front matter
PII: S1566-1199(02)00033-2

interface mechanisms, and the bulk Fermi level position, which is defined by doping). Carrier tunneling through the narrow depletion region increases injection. Additional flexibility can also be expected at the level of the energy barrier itself, which is likely to exhibit a larger dependence on doping than barriers at inorganic semiconductor interfaces where bonding, and thus anchoring of energy levels, is stronger.

Doping of metal–organic contacts with inorganic donors, such as lithium in Alq_3 [1–4] or BCP [5], and acceptors, such as antimony pentachloride in TPD [6] or iron trichloride in α-NPD [7], has shown potential for significant improvement in current injection. Doping with molecular acceptors, e.g. tetracyanoquinodimethane (TCNQ) and its fully fluorinated derivative tetrafluorotetracyanoquinodimethane (F_4-TCNQ) [8–12], and molecular donors, e.g. BEDT-TTF (bis(ethylenedithio)-tetrathiafulvalene) [13] has shown equally impressive possibilities and has recently led to record breaking turn-on voltages in an OLED [11]. Considerable work remains to be done, however, to understand and control doping in materials which exhibit fundamental differences with standard inorganic semiconductors. In particular, the weak intermolecular bonds, large energy gaps and small dielectric constants of these materials are not particularly conducive to low dopant ionization energies. Several groups have started to investigate doping mechanisms and their effects on the electronic structure of the host organic molecular films [12,14–17]. Particularly important are the relative energies of dopant and host molecular levels, which determine the "ionization energy" and doping efficiency. Blochwitz et al. [14] reported the first ultra-violet photoemission spectroscopy (UPS) study of electronic levels and Fermi energy position in films of zinc phthalocyanine (ZnPc) doped with the molecular acceptor F_4-TCNQ. We recently investigated the same system using UPS, inverse photoemission spectroscopy (IPES), X-ray photoemission spectroscopy (XPS) and in situ current–voltage measurements (I–V) [12]. In agreement with the results of Blochwitz et al. [14], we showed that the Fermi level (E_F) drops from a near mid-gap position in undoped ZnPc to 0.18 eV above the highest occupied molecular orbital (HOMO) in 3% doped films. We measured the filled and empty states of the host and guest molecules, and showed that the electron affinity of the dopant F_4-TCNQ molecule (5.24 eV) and ionization energy of the host ZnPc molecule (5.28 eV) are compatible with a direct electron transfer from the HOMO of ZnPc to the lowest unoccupied molecular orbital (LUMO) of F_4-TCNQ. This electron transfer is further analyzed in the present paper with an IPES investigation of the evolution of the F_4-TCNQ empty states upon capture of electrons from ZnPc molecules.

Our initial study of ZnPc:F_4-TCNQ [12] also showed an increase of several orders of magnitude in current injected in the doped films with respect to the undoped films, consistent with an increase in the concentration of free holes. The present paper expands on this preliminary analysis by addressing the specific issue of whether the doping-induced increase in current in Au/ZnPc/Au devices is due predominantly to an increase in carrier injection, i.e. via tunneling through the thin depletion region of the doped interface, or to an increase in the bulk conductivity of the film. The resolution of this issue in the ZnPc:F_4-TCNQ system presents some difficulties because of the rapid diffusion of the dopant in the host film [12]. Diffusion prevents doping the interface region of the organic film only, and complicates the assessment of increase in interface injection versus bulk conductivity. We address this issue here with an investigation of the current injected as a function of the thickness of the organic film. We show that the I–V characteristics of Au/(undoped)ZnPc/Au devices with different ZnPc thickness correspond to an injection-limited current. This current is described in terms of thermionic emission with a smaller injection rate pre-factor A^* than predicted by the Richardson constant. On the other hand, the I–V characteristics of Au/ZnPc:0.3%F_4-TCNQ/Au devices exhibit a transition from injection-limited to bulk-limited current transport at a critical electric field F_C related to the thickness of the organic film. For $F > F_C$, the current is adequately described in terms of trap-free space-charge-limited conduction (SCLC) with a field-dependent mobility. The current is almost seven orders of magnitude larger for the ZnPc:0.3%F_4-TCNQ devices than for the undoped

ZnPc devices. This increase is the result of enhanced carrier injection via tunneling through the narrow space charge layer of the doped interface.

2. Experimental

All the experiments were performed in an ultra-high vacuum (UHV) system consisting of three interconnected chambers equipped for surface preparation, device growth and testing, and surface/interface analysis (UPS, IPES, XPS). The substrates were Si (1 0 0) wafers pre-coated with ~200 Å Cr and 800 Å Au. Both organic materials were purchased from Sigma-Aldrich. ZnPc was purified via three cycles of gradient sublimation prior to insertion in the UHV system, then placed in an evaporation cell in the preparation chamber (base pressure 2×10^{-10} Torr) and extensively outgassed. The ex situ purification of ZnPc is particularly important to insure that the undoped material is intrinsic. On the other hand, in view of the relatively small amount of F_4-TCNQ available for this experiment, the dopant was not purified by gradient sublimation, and was only thoroughly outgassed in UHV. This short cut has negligible consequences on the doping of ZnPc because only a small fraction of a percent of impurities are ultimately incorporated in the doped layer. On the other hand, the presence of impurities in F_4-TCNQ may explain the measured position of the Fermi level in pure films of this material, as discussed in the next section. Between growth sequences, evaporation cells were maintained at a temperature slightly below the material sublimation temperature to continuously outgass the load. The deposition rates from the two thermally shielded organic sources were monitored with a quartz crystal microbalance, using 1.5 g/cm^3 as the bulk density for ZnPc and 1.4 g/cm^3 for F_4-TCNQ.

The electronic properties of pure ZnPc and F_4-TCNQ were measured at the surface of neat 100 Å thick films deposited on Au. The ZnPc films were deposited at room temperature, while the F_4-TCNQ films were deposited at −20 °C to increase the sticking coefficient. All measurements were done at room temperature. Both compounds displayed excellent stability under photon and electron irradiation for UPS and IPES data collection times in excess of 30 min. The electronic structure of the ZnPc/Au interface was measured by UPS following incremental depositions of organic material on the metal substrate. The doped ZnPc:F_4-TCNQ films were deposited by co-evaporation using growth rates of 1–2 Å/s for ZnPc and 0.2–1 Å/min for F_4-TCNQ to obtain molar doping ratios of 0.3% and 3%. Because of the very low dopant evaporation rate used for the 0.3% films, the molecular ratio of these films is to be trusted to within a factor of 5 only.

Measurements of filled and empty states and onset of photoemission (for determining the vacuum level [18]) were obtained following a standard methodology of incremental build-up of a film alternating with UPS and IPES measurements. The energy position of the HOMO and LUMO were determined with respect to the Fermi level (E_F), measured separately on the Au substrate, and to the vacuum level (E_{vac}) of the film. The ionization energy and electron affinity of the condensed organic film are conventionally defined as the energy difference between E_{vac} and the leading edges of the HOMO and LUMO, respectively. The energy scales of the UPS and IPES spectra were aligned by matching the Fermi energies obtained from the Au substrate. The resolution of the UPS and IPES measurements were 0.15 and 0.45 eV, respectively [19]. All the experiments described here were performed under conditions of negligible charging or surface photovoltage during electron spectroscopy.

I–V measurements were carried out in situ at room temperature on Au/ZnPc/Au devices consisting of a 400 Å thick Au metal base, an undoped or doped (0.3%) ZnPc film with thickness ranging between 1400 and 7400 Å, and 400 Å thick top Au electrodes evaporated through a shadow mask defining an array of 0.78, 0.13 and 0.0078 mm^2 round apertures.

3. Results and discussion

3.1. Electronic structure of films and interfaces

Composite UPS/IPES spectra of filled and empty states of ZnPc and F_4-TCNQ neat films are

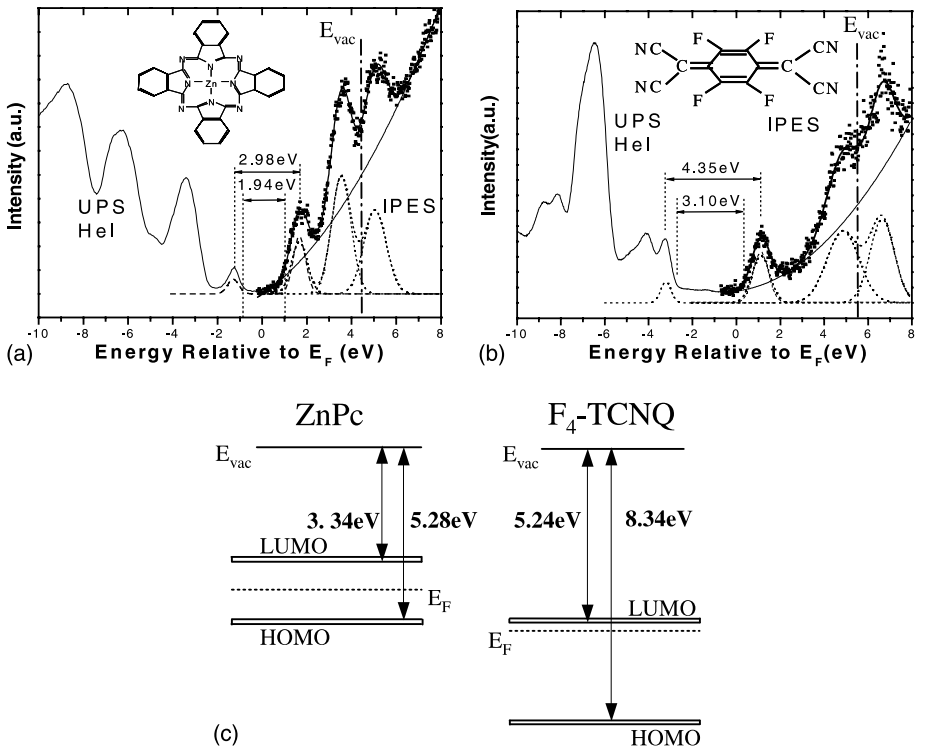

Fig. 1. Combined UPS–IPES spectra of a 100 Å thick film of (a) ZnPc and (b) F_4-TCNQ. Insets show the chemical structure of the two molecules. (c) Ionization energy and electron affinity of the ZnPc and F_4-TCNQ films deduced from the UPS and IPES measurements.

shown in Fig. 1(a) and 1(b). HOMO and LUMO peaks at −1.3 and +1.8 eV for ZnPc and −3.2 and +1.1 eV for F_4-TCNQ, respectively, are well resolved for both compounds. The electronic structures of pure ZnPc and F_4-TCNQ films are summarized in Fig. 1(c). The ionization energy and electron affinity of ZnPc are 5.28 and 3.34 eV, respectively, giving an edge-to-edge gap of 1.94 eV similar to that of CuPc [20]. The ionization energy and electron affinity of F_4-TCNQ are 8.34 and 5.24 eV, respectively. These values are among the highest reported for π-conjugated molecular films [21,22], indicating that F_4-TCNQ is likely to act as an acceptor in a number of molecular compounds. In that regard, the residual impurities present in the F_4-TCNQ film as a result of the by-pass of the gradient purification step, are likely to act as donors. They presumably cause the observed "pinning" of E_F close to the LUMO in the F_4-TCNQ film (Fig. 1(b) and (c)). However, we do not expect any significant impact of the small amount of impurities present in the F_4-TCNQ source material on the doping of ZnPc.

The match between the ZnPc ionization energy and the F_4-TCNQ electron affinity suggests an energetically favorable electron transfer from the host to the dopant, resulting in efficient p-type doping. One should note, however, that the electron affinity of F_4-TCNQ is measured for molecules in a pure F_4-TCNQ film, i.e. a molecular environment that is different from that encountered by F_4-TCNQ molecules dispersed in ZnPc. The direct comparison of the electron affinity of the guest and ionization energy of the host, done above to assess doping efficiency, makes the implicit assumption that the polarization experienced by the negatively charged F_4-TCNQ molecular ion created by IPES [23] is the same in the two environments. This assumption is generally valid to within a few tenth of an eV for a number of molecular compounds [21].

The ZnPc-to-F_4-TCNQ charge exchange expected from the relative positions of the host HOMO and dopant LUMO is unambiguously demonstrated by the UPS and IPES spectra recorded as a function of ZnPc deposition on a film of F_4-TCNQ (Fig. 2). The clean F_4-TCNQ film displays a strong LUMO peak (arrow at 1.1 eV) which is rapidly attenuated upon deposition of ZnPc, indicative of the filling of the lowest empty state of the substrate with electrons from the overlayer molecules. The higher F_4-TCNQ empty states remain basically unaffected, except for the growth of the ZnPc LUMO peak at ~2.5 eV. On the side of the filled states, the F_4-TCNQ HOMO (−3.2 eV) is rapidly masked by the intense ZnPc HOMO − 1 peak, while the former F_4-TCNQ gap is progressively filled by the ZnPc HOMO (~−0.7 eV).

The UPS spectra of undoped ZnPc grown on Au as a function of layer thickness is shown in Fig. 3(a), and the electronic structure of the ZnPc/Au interface is summarized in Fig. 4(a). The abrupt shift of the vacuum level (left part of panel (a)) upon deposition of the first molecular layer of ZnPc (~4–8 Å) indicates the formation of a 0.76

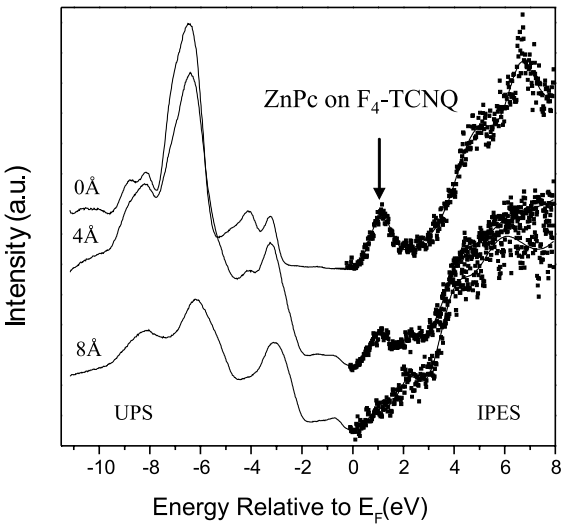

Fig. 2. Combined UPS–IPES spectra of an F_4-TCNQ film as functions of incremental deposition of ZnPc. The arrow marks the IPES feature corresponding to the F_4-TCNQ LUMO, which is rapidly attenuated upon filling by ZnPc electrons. Other features are described in the text.

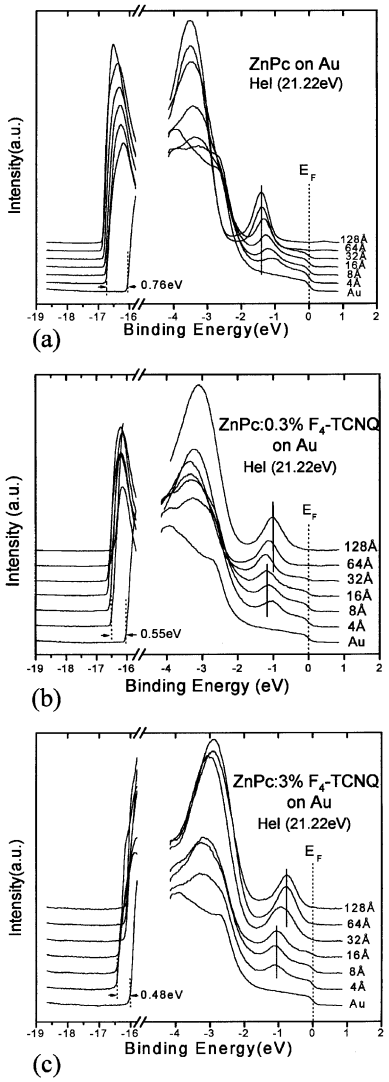

Fig. 3. UPS spectra of ZnPc films incrementally deposited on Au: (a) pure ZnPc; (b) ZnPc:0.3%F_4-TCNQ; (c) ZnPc:3%F_4-TCNQ. The right part of each spectrum represents the low binding energy states, including the HOMO, and the left part represents the onset of photoemission, corresponding to the vacuum level.

eV interface dipole barrier. In spite of the close match between the Au work function and the ZnPc ionization energy, the interface hole barrier is large (~0.9 eV). This interface belongs to the large group of organic/metal interfaces at which the vacuum level alignment rule, or Schottky–Mott limit, breaks down [24,25]. The sign of the

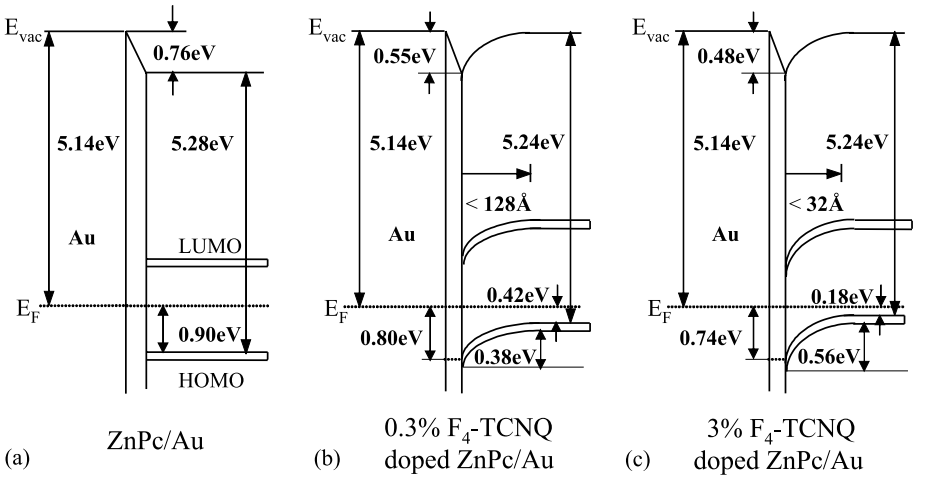

Fig. 4. Energy of molecular levels near the interface between Au and (a) undoped ZnPc; (b) ZnPc:0.3%F_4-TCNQ; (c) ZnPc:3%F_4-TCNQ. The measured width of the depletion region is shown in (b) and (c). Interface dipole, work function of Au and ZnPc ionization energy are indicated in each case.

dipole suggests a (partial) electron transfer from the organic material to the metal. Alternatively, a decrease in the metal work function, resulting from the compression of the tail of the electronic wave function at the metal surface by adsorbed molecules has also been invoked to explain this type of dipole [26]. The vacuum and all other molecular levels are flat away from the interface within experimental error, consistent with results obtained for the majority of organic-on-metal interfaces investigated to date [27]. The HOMO gradually shifts to higher binding energy, indicating an evolution of the measured ZnPc ionization potential from 5.12 eV at 4 Å to 5.28 eV at 64 Å and above, in accord with the change in polarization screening from the organic–metal interface to the surface of the thick organic film [28]. E_F is near mid-gap at 0.90 eV above the leading edge of ZnPc HOMO, indicative of the electrically intrinsic character of pure ZnPc.

The UPS spectra of ZnPc:0.3%F_4-TCNQ deposited on Au are shown in Fig. 3(b) and the corresponding interface electronic structure is summarized in Fig. 4(b). The dopant concentration is assumed to be constant throughout the ZnPc film. The interface dipole is reduced by 0.2 eV with respect to the undoped case. F_4-TCNQ molecules close to the interface exert a strong electron attraction which tends to reduce the electron transfer from the organic layer to the metal and the decrease of the metal work function due to the perturbation of the metal surface electronic tail. The ionization energy of the thin (~monolayer) doped film is also ~80 meV higher than that of the thin undoped film. The difference is not understood at this point, however it is close to experimental resolution and may not be significant. The UPS spectra show a 0.3–0.4 eV shift of the HOMO and other UPS features toward lower binding energy with increasing layer thickness up to 128 Å, indicative of an upward molecular level bending away from the interface. The bulk position of the leading edge of the HOMO is 0.42 eV below E_F, i.e. 0.48 eV closer than in undoped ZnPc. The thickness of the space charge region is estimated to be about 120 Å, corresponding to 30–40 molecular planes assuming that the molecules are stacked with their plane parallel to the substrate surface. The ionization potential of the 128 Å film (5.24 eV) is equal to that of the undoped film at the same thickness within experimental error, suggesting that the growth mode of the doped films is similar to that of the undoped film despite the incorporation of the dopant molecules.

The UPS spectra and electronic structure of the ZnPc:3%F_4-TCNQ/Au interface are shown in

Figs. 3(c) and 4(c). The interface dipole is now reduced by nearly 0.3 eV with respect to the undoped interface, consistent with an increasing effect of interface dopant molecules on charge transfer and/or modification of the metal surface electronic structure. The UPS spectra show a 0.5–0.6 eV shift of the valence states toward lower binding energy with increasing layer thickness up to 30–40 Å, indicative of an increased upward molecular level bending away from the interface. The leading edge of the doped ZnPc HOMO is 0.18 eV below E_F in the bulk of the film, i.e. 0.72 eV closer than in undoped ZnPc. The thickness of the space charge region is estimated at 30–40 Å. The ionization potential of the doped film (5.24 eV) is equal to that of the 0.3% doped film and undoped film within experimental error.

As expected, the 3% doping leads to a larger molecular level bending, a bulk HOMO position closer to E_F, and a narrower space charge region than the 0.3% doping. Assuming a dielectric constant $\varepsilon = 3$ in the organic film, a charge transfer ratio between host and dopant molecules equal to 1 and a standard electrostatic model, the width of the depletion region is estimated at 20 Å for ZnPc:3%F_4-TCNQ film and 52 Å for ZnPc: 0.3%F4-TCNQ, in fair agreement with the experimental estimations of 30–40 and 100–120 Å, respectively. The discrepancy between measured and expected thickness could be due to a slight overestimation (by a factor of 1.5–2) of the incorporation of dopant molecules in the ZnPc film, or to a systematic error in the thickness of the film due to a non-unity sticking coefficient of the molecules.

3.2. Current injection in doped ZnPc: bulk versus interface effects

Charge injection into ZnPc is analyzed for the undoped and 0.3% doped films only, the currents measured for the 3% doped films being excessively large for our experimental set-up. Further discussion of this point will be given at the end of this section. The hole injection barriers measured by UPS are 0.90 and 0.80 eV for the undoped and 0.3% doped films deposited on Au, respectively. Like for the interface dipole, this difference presumably comes from an increase in the density of electrons due to acceptor molecules at the interface, which raises the energy levels of the organic material with respect to the Fermi level of the metal. The room temperature I–V characteristics measured in situ for Au/ZnPc/Au and Au/ZnPc:0.3%F_4-TCNQ/Au of various organic layer thickness are shown in Fig. 5(a) and 5(b), respectively. All the I–V curves correspond to holes injected from the bottom Au electrode. The current is nearly seven orders of magnitude larger for the doped than for the undoped device. This difference cannot be explained by the 0.1 eV change in

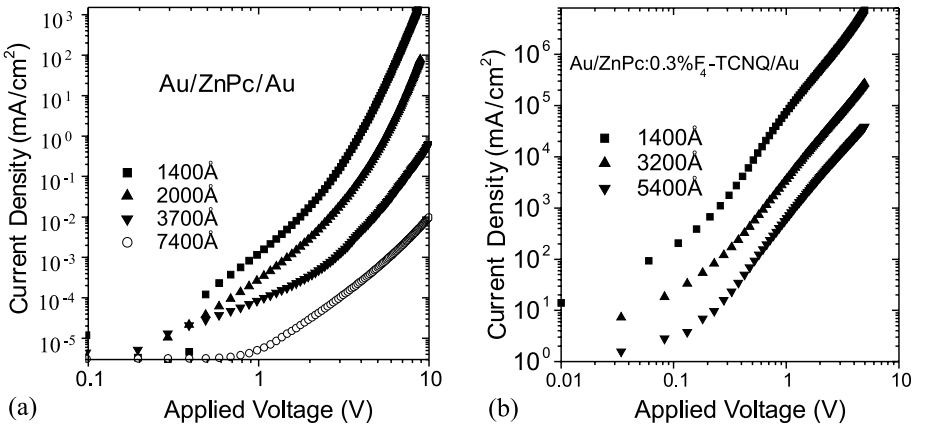

Fig. 5. Thickness dependence of I–V characteristics measured in situ for Au/ZnPc/Au structures: (a) undoped ZnPc; (b) ZnPc:0.3%F_4-TCNQ.

barrier height, and must be due to an increase in film conductivity or in carrier injection via tunneling, or both. Which of the two mechanisms dominates depends on whether the current is injection- or bulk-limited. The analysis of the current injected in a device where only the interface region is doped should provide an answer to this question, however the rapid diffusion of F_4-TCNQ in ZnPc precludes "local" doping in this system [12]. We circumvent this problem here by analyzing the dependence of the current on the thickness of the organic film [29]. To aid in the discussion, we briefly review generic injection-limited or transport-limited cases before focusing on the experimental results.

In the case of a purely injection-limited current, and regardless of the specific limiting mechanism, the current at constant field F has no explicit thickness dependence,

$$j = j(F). \tag{1}$$

The carrier injection into a semiconductor is usually treated either in terms of Richardson–Schottky (RS) thermionic emission or Fowler–Nordheim (FN) tunneling [30]. The RS model is based on the lowering of barrier by the image charge potential under an external field $F = V/d$. The current density j_{RS} as a function of the field is given by

$$j_{RS} = A^* T^2 \exp\left(-\frac{\phi_B - \beta_{RS}\sqrt{F}}{k_B T}\right), \tag{2}$$

where $A^* = 4\pi q m^* k_B^2/h^3$ (= 120 A/cm^2 K^2 for $m^* = m_0$) is the Richardson constant, $\beta_{RS} = \sqrt{q^3/4\pi\varepsilon\varepsilon_0}$ and ϕ_B is the zero-field injection barrier. On the other hand, the tunneling model ignores Coulombic effects and considers tunneling through a triangular barrier into a continuum of states,

$$j_{FN} = \frac{A^* q^2 F^2}{\phi_B \alpha^2 k_B^2} \exp\left(-\frac{2\alpha\phi_B^{3/2}}{3qF}\right). \tag{3}$$

Both models are, under certain conditions, appropriate in inorganic semiconductors with extended band states and large mean free path. However, injection into disordered systems, in which transport involves carrier hopping, leads to enhanced backflow of injected carriers into the electrode. Monte-Carlo simulations [31] show that, although this type of injection resembles RS thermionic emission, quantitative differences exist regarding the field and temperature dependence of the current. The absolute value of the current is also found to be orders of magnitude lower than predicted by the Richardson constant.

In the case of trap-free SCLC with or without field-dependent mobility, the current at constant field scales as d^{-1},

$$j = j(F)/d. \tag{4}$$

Specifically, if a field-independent mobility is assumed, the SCLC obeys the Mott–Gurney equation [32].

$$j_{SCLC} = \frac{9}{8}\varepsilon\varepsilon_0\mu\frac{V^2}{d^3}. \tag{5}$$

For a field-dependent mobility, which is often observed in amorphous molecular materials, molecularly doped polymers and most conjugated polymers, Murgatroyd [33] derived an approximate analytical expression of the mobility, i.e. the Poole–Frenkel (PF) field dependence of the mobility,

$$\mu(F) = \mu_0 \exp\left(\beta\sqrt{F}\right), \tag{6}$$

and of the current density,

$$j_{SCLC} = \frac{9}{8}\varepsilon\varepsilon_0\mu_0\frac{V^2}{d^3}\exp\left(0.89\beta\sqrt{V/d}\right). \tag{7}$$

Finally, for trap-charge-limited conduction (TCLC) with an exponential trap distribution and a field-independent mobility, the current at constant field scales as d^{-l} with $l > 1$ [34,35],

$$j = j(F)/d^l. \tag{8}$$

Like for TCLC, the SCLC with a PF field dependence of the mobility can also yield a power law behavior (with a power larger than 2) of the current versus voltage. Fortunately, the difference in the thickness dependence of these two mechanisms helps distinguish between them.

The current injected in undoped ZnPc as a function of field is shown in Fig. 6(a). The current

is clearly independent of film thickness, demonstrating that it is injection-limited at least for film thickness up to 7400 Å and fields up to 0.4×10^6 V/cm. To evaluate the correspondence between these I–V measurements and the injection barrier measured by UPS, we calculate the current versus electric field using the thermionic emission (RS) model. According to Eq. (2), $\log j_{RS}$ versus $\sqrt{F}$ is a straight line with a Y-axis intercept equal to $\log A^* T^2 - \log e\phi_B/k_B T$ and a slope equal to $\beta_{RS} \log e/k_B T$. As shown in Fig. 6(b), the reduced experimental data indeed follow a straight line over many orders of magnitude. The slope of the linear fit gives $\beta_{RS} = 1.125 \times 10^{-22}$ $(\text{cm/V})^{1/2}$, which is larger by a factor of 3 than the coefficient predicted by the RS model ($\beta_{RS} = 3.504 \times 10^{-23}$ $(\text{cm/V})^{1/2}$). The 0.9 eV injection barrier obtained by UPS leads to a RS constant $A^* = 8.9$ A/cm^2 K^2, which is roughly an order of magnitude smaller than the standard value $A^* = 120$ A/cm^2 K^2 predicted by the classical RS theory, but consistent with the fact that in hopping injection, injected carriers can be scattered due to the disorder and return to the electrode, as claimed by Wolf et al. [31].

The analysis of the I–V characteristics of pure ZnPc devices in terms of FN tunneling model is shown in Fig. 6(c). According to Eq. (3), $\log j/F^2$ versus F^{-1} should yield a straight line, which is clearly not the case. It suggests that tunneling is not involved at relatively low electric field, in agreement with Monte-Carlo simulations [31] which demonstrate the irrelevance of long-range tunneling transitions for various jumping distances between the metal and the adjacent layer of the amorphous organic dielectric.

The thickness dependence of the current versus electric field in 0.3% doped devices is shown in Fig. 7(a) for organic film thickness ranging between 1400 and 5400 Å. For electric fields lower than 0.03×10^6 V/cm, the current is independent of thickness, and thus still injection-limited. At higher electric fields, the current shows a clear dependence on thickness. When reploted as (current density × layer thickness) versus electric field (Fig. 7(b)), the three curves collapse into one when the electric field exceeds 0.06×10^6 V/cm, demonstrating perfect trap-free SCLC behavior according to

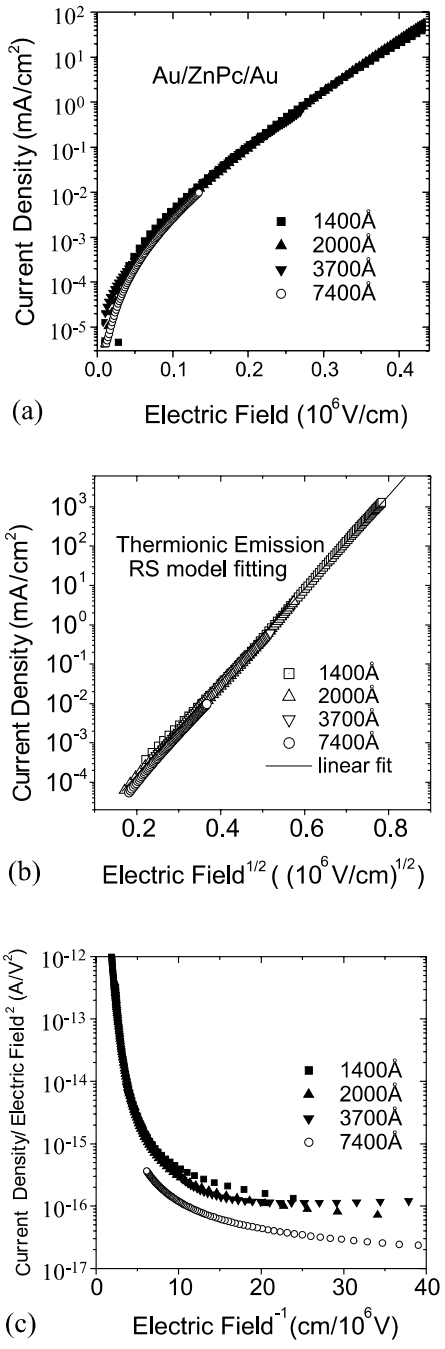

Fig. 6. I–V characteristics of Au/undoped ZnPc/Au structures as functions of ZnPc thickness: (a) current density versus electric field; (b) current density versus (electric field)$^{1/2}$ compared to the thermionic emission (RS) model; (c) current density/(electric field)^2 versus (electric field)$^{-1}$ in terms of tunneling (FN) model fitting.

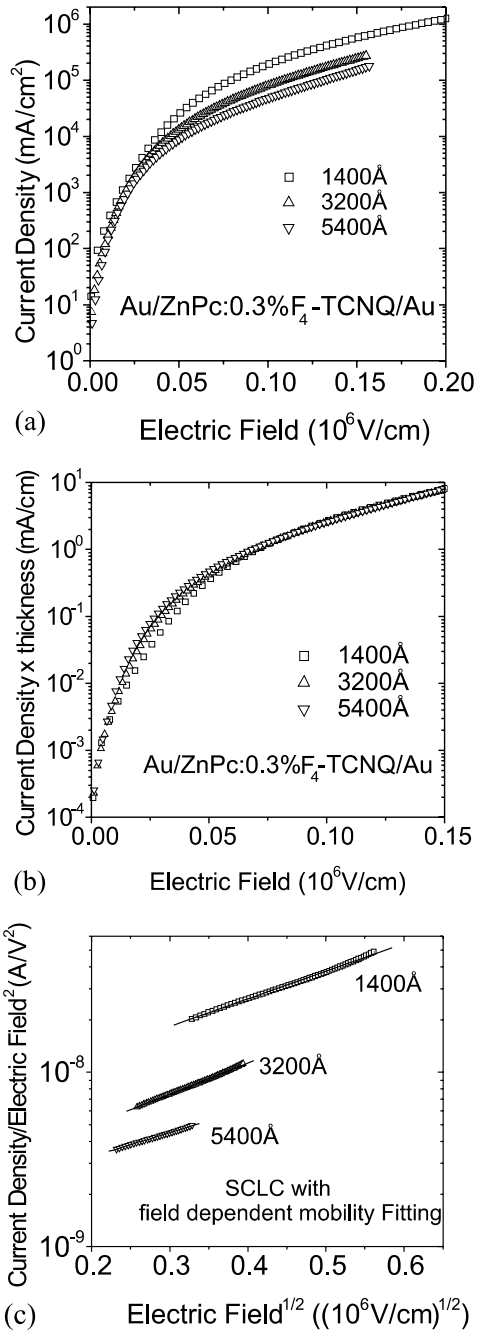

Fig. 7. *I–V* characteristics of Au/ZnPc:0.3%F_4-TCNQ/Au structure with different organic layer thickness: (a) current density versus electric field; (b) current density × thickness versus electric field; (c) current density/(electric field)^2 versus (electric field)$^{1/2}$ in terms of SCLC with field dependent mobility fitting.

Eq. (4). Furthermore, the critical electric field for onset of SCLC decreases as the organic layer thickness increases, consistent with the fact that SCLC scales with F/d (assuming that the interface property has no dependence on the layer thickness).

This analysis demonstrate that the interface carrier injection limits the current in the pure ZnPc device, while the current is limited by the bulk conductivity in the 0.3% doped device. We conclude therefore that the large improvement in current upon doping is the result of improved hole injection via tunneling through the thin space charge region, since the interface injection barrier remains nearly unchanged as confirmed by the UPS study.

We now return to the issue of the excessive current in the 3% doped film mentioned at the beginning of Section 3.2. If the current is space-charge-limited, no dependence on doping should be observed. However, the electric field necessary to reach SCLC is proportional to the density of charge carriers, and thus increases by an order of magnitude when the dopant concentration is increased from 0.3% to 3%. Our *I–V* measurements are limited to 0–10 V and thus do not reach the SCLC regime in the 3% doped film. The current is therefore still limited by injection and/or ohmic conduction, and both are larger than in the 0.3% film, because of the narrower space charge region and higher current density.

Finally, the *I–V* characteristics of the 0.3% doped ZnPc device in the SCLC regime are fitted in Fig. 7(c) with the trap-free SCLC model (since $j \propto j(F)/d$, Eq. (7)) including a PF type mobility $\mu(F) = \mu_0 \exp(\beta\sqrt{F})$. According to Eq. (7), the current should yield a linear dependence of $\log j/F^2$ on $\sqrt{F}$. The three curves obey this dependence, yielding nearly identical slopes equal to $0.89\beta \log e = 1.782 \times 10^{-4}$ (m/V)$^{1/2}$ and *Y*-axis intercepts equal to $(\log 9/8)(\varepsilon\varepsilon_0\mu_0/d)$. The slope and intercept of the three curves give $\beta = (4.09 \pm 0.53) \times 10^{-3}$ (cm/V)$^{1/2}$ and a low-field mobility $\mu_0 = 0.279 \pm 0.044$ cm^2/V s. The value of β is comparable to those usually found for organic films [36]. The low field mobility is high, but in line with mobilities expected for polycrystalline films of phthalocyanines [37].

4. Summary

We demonstrated that p-type doping of ZnPc with F_4-TCNQ results from an efficient electron transfer due to an excellent match between ionization energy of the host molecule and the electron affinity of the dopant. The Fermi level is found at 0.42 and 0.18 eV above the edge of the HOMO level in the bulk of the 0.3% and 3% doped films, respectively, indicating strong p-type character. Doping leads to the formation of a narrow space charge region (100–120 Å for 0.3% doping and 30–40 Å for 3% doping) at the ZnPc/Au interface. In situ transport measurements show an increase by seven orders of magnitude in the current injected in Au/ZnPc:0.3%F_4-TCNQ/Au structures with respect to the current injected in the undoped layers. The analysis of the dependence of the current on the thickness of the organic layer indicates that the current increase is due to tunneling through the narrow interface depletion region.

Acknowledgements

Support of this work by the NSF (DMR-0097133) and by the New Jersey Center for Optoelectronics is gratefully acknowledged.

References

[1] J. Kido, T. Matsumoto, Appl. Phys. Lett. 73 (1998) 2866.
[2] M.G. Mason, C.W. Tang, L.-S. Hung, P. Raychaudhuri, J. Madathil, D.J. Giesen, Y. Yan, Q.T. Le, Y. Gao, S.-T. Lee, L.S. Liao, L.F. Cheng, W.R. Salaneck, D.A. dos Santos, J.L. Brédas, J. Appl. Phys. 89 (2001) 2756.
[3] C. Ganzorig, M. Fujihira, Jpn. J. Appl. Phys. 38 (1999) L1348.
[4] C. Ganzorig, K. Suga, M. Fujihira, Mat. Sci. Eng. B-Solid 85 (2001) 140.
[5] G. Parthasarathy, C. Shen, A. Kahn, S.R. Forrest, J. Appl. Phys. 89 (2001) 4986.
[6] C. Ganzorig, M. Fujihira, Appl. Phys. Lett. 77 (2000) 4211.
[7] J. Kido, in: Proceedings of IUMRS-ICA, Hong Kong, July 2000.
[8] J. Blochwitz, M. Pfeiffer, T. Fritz, K. Leo, Appl. Phys. Lett. 73 (1998) 729.
[9] M. Pfeiffer, T. Fritz, J. Blochwitz, A. Nollau, B. Plönnigs, A. Beyer, K. Leo, Adv. Solid State Phys. 39 (1999) 77.
[10] M. Pfeiffer, A. Beyer, T. Fritz, K. Leo, Appl. Phys. Lett. 73 (1998) 3202.
[11] X. Zhou, M. Pfeiffer, J. Blochwitz, A. Werner, A. Nollau, T. Fritz, K. Leo, Appl. Phys. Lett. 78 (2001) 410.
[12] W. Gao, A. Kahn, Appl. Phys. Lett. 79 (2001) 4040.
[13] A. Nollau, M. Pfeiffer, T. Fritz, K. Leo, J. Appl. Phys. 87 (2000) 4340.
[14] J. Blochwitz, T. Fritz, M. Pfeiffer, K. Leo, D.M. Alloway, P.A. Lee, N.R. Armstrong, Organic Electronics 2 (2001) 97.
[15] N. Koch, A. Rajagopal, J. Ghijsen, R.L. Johnson, G. Leising, J.-J. Pireaux, J. Phys. Chem. B 104 (2000) 1434.
[16] N. Koch, A. Rajagopal, E. Zojer, J. Ghijsen, X. Crispin, G. Pourtois, J.-L. Bredas, J.-J. Pireaux, G. Leising, Surf. Sci. 454–456 (2000) 1000.
[17] C. Shen, A. Kahn, J. Appl. Phys. 90 (2001) 4549.
[18] I.G. Hill, A. Rajagopal, A. Kahn, J. Appl. Phys. 84 (1998) 3236.
[19] C.I. Wu, Y. Hirose, H. Sirringhaus, A. Kahn, Chem. Phys. Lett. 272 (1997) 43.
[20] I.G. Hill, A. Kahn, J. Appl. Phys. 86 (1999) 2116.
[21] N. Sato, K. Seki, H. Inokuchi, J. Chem. Soc. Faraday Trans. 77 (2) (1981) 1621.
[22] K. Sugiyama, D. Yoshimura, T. Miyamae, T. Miyazaki, H. Ishii, Y. Ouchi, K. Seki, J. Appl. Phys. 83 (1998) 4928.
[23] I.G. Hill, A. Kahn, Z.G. Soos, R.A. Pascal Jr., Chem. Phys. Lett. 327 (2000) 181.
[24] H. Ishii, K. Seki, IEEE Trans.Electron. Dev. 44 (1997) 1295.
[25] I. Hill, A. Rajagopal, A. Kahn, Y. Hu, Appl. Phys. Lett. 73 (1998) 662.
[26] H. Ishii, K. Sugiyama, E. Ito, K. Seki, Adv. Mater. 8 (1999) 605.
[27] I.G. Hill, J. Schwartz, A. Kahn, Org. Electron. 1 (2000) 5.
[28] I.G. Hill, A.J. Mäkinen, Z.H. Kafafi, Appl. Phys. Lett. 77 (2000) 1825.
[29] W. Brütting, S. Berleb, A.G. Mückl, Organic Electronics 2 (2001) 1.
[30] S.M. Sze, Physics of Semiconductor Devices, Wiley, New York, 1981.
[31] U. Wolf, V.I. Arkhipov, H. Bässler, Phys. Rev. B 59 (1999) 7507.
[32] N.F. Mott, R.W. Gurney, in: Electronic Processes in Ionic Crystals, Clarendon Press, Oxford, 1940.
[33] P.N. Murgatroyd, J. Phys. D: Appl. Phys. 3 (1970) 151.
[34] M.A. Lampert, P. Mark, Current Injection in Solids, Academic Press, New York, 1970.
[35] K.C. Kao, W. Hwang, Electrical Transport in Solids, Pergamon Press, Oxford, 1981.
[36] W. Brütting, H. Riel, T. Beierlein, W. Riess, J. Appl. Phys. 89 (2001) 1704.
[37] M. Pope, C. Swenberg, Electronic Processes in Organic Crystals and Polymers, second ed., Oxford University Press, Oxford, 1999, p. 670.